Mon. Not. R. Astron. Soc. **321**, 733–742 (2001)

Chemo-spectrophotometric evolution of spiral galaxies – IV. Star formation efficiency and effective ages of spirals

S. Boissier,[1] A. Boselli,[2] N. Prantzos[1★] and G. Gavazzi[3]

[1]*Institut d'Astrophysique de Paris, 98bis Bd. Arago, 75104 Paris, France*
[2]*Laboratoire d'Astronomie Spatiale, Traverse du Siphon, F-13376 Marseille Cedex 12, France*
[3]*Università degli Studi di Milano – Bicocca, Pizza dell'Ateneo Nuovo 1, 20126 Milano, Italy*

Accepted 2000 September 15. Received 2000 September 15; in original form 2000 April 20

ABSTRACT

We study the star formation history of normal spirals by using a large and homogeneous data sample of local galaxies. For our analysis we utilize detailed models of chemical and spectrophotometric galactic evolution, calibrated on the Milky Way disc. We find that star formation efficiency is independent of galactic mass, while massive discs have, on average, lower gas fractions and are redder than their low-mass counterparts; put together, these findings convincingly suggest that massive spirals are older than low-mass ones. We evaluate the effective ages of the galaxies of our sample and we find that massive spirals must be several Gyr older than low-mass ones. We also show that these galaxies (having rotational velocities in the 80–400 $\mathrm{km\,s^{-1}}$ range) cannot have suffered extensive mass losses, i.e. they cannot have lost during their lifetime an amount of mass much larger than their current content of gas+stars.

Key words: galaxies: evolution – galaxies: general – galaxies: photometry – galaxies: spiral – galaxies: stellar content.

1 INTRODUCTION

The star formation rate (SFR) is the most important and the least well-understood ingredient in studies of galaxy evolution. Despite more than 30 yr of observational and theoretical work, the Schmidt law still remains popular among theoreticians and compatible with most available observations (e.g. Kennicutt 1998a).

It is well known that there are systematic trends in the star formation (SF) history of the Hubble sequence: The ratio $\Psi/\langle\Psi\rangle$ of the current SFR Ψ to the past average one $\langle\Psi\rangle$ (integrated over the age of the galaxy) increases as one goes from early- to late-type galaxies, albeit with a large dispersion within each morphological type. The Hubble sequence seems to be determined by the characteristic time-scale for star formation, with early-type galaxies forming their stars in shorter time-scales than those of late types. However, this simple description of the Hubble sequence fails to answer two important, and probably related, questions: (i) What determines the characteristic time-scale for SF in galaxies? (ii) What is the role (if any at all) of the mass of a galaxy?

Gavazzi, Pierini & Boselli (1996) found an anticorrelation between the SFR per unit total mass and galactic luminosity; part of this trend may reflect the aforementioned dependence of SFR on Hubble type, but it may also be that this trend is fundamentally related to the galactic mass. In a recent work Bell & de Jong (2000) use a large sample of spiral galaxies with resolved optical and near-infrared photometry and find that it is rather surface density that drives the star formation history of galaxies, while mass is a less important parameter.

Photometric studies alone cannot lift the age–metallicity degeneracy, namely the fact that young and metal-rich stellar populations may be redder than old and metal-poor ones. Studies of the chemical aspects of galaxy evolution (i.e. gas fractions, star formation rates, metal abundances) can help to tackle the problem from a different angle, but they are also limited by the unknown history of gaseous flows from and to the system. A study combining elements from both photometric and chemical evolution offers the best chances to understand this complex situation.

In this work we study the star formation history of spirals by using detailed models of chemical and spectrophotometric galactic evolution. The numerical code has been presented in detail elsewhere (Boissier & Prantzos 1999, hereafter Paper I) and is only briefly described in Section 2. It has been successfully applied to the modelling of global properties of spirals (Boissier & Prantzos 2000, hereafter Paper II), as well as to the corresponding abundance and photometric gradients (Prantzos & Boissier 2000, hereafter Paper III). Based on the recent work of Boselli et al. (2001), we use here a large and homogeneous sample of data for normal spirals (presented in Section 3), ideally suited for the purpose of this work. Our results and the comparison with the observations are presented in Section 4. They suggest that galactic mass is the main driver of galactic evolution, although local

★ E-mail: prantzos@iap.fr

surface density may also play a role. We argue that massive galaxies are, on average, older than less massive ones, based on the fact that star formation efficiencies seem to be independent of galactic mass, while gas fractions are systematically low in massive spirals. Based on the observed star formation efficiencies and gas fractions, we derive in Section 5 corresponding galactic ages by using simple analytical models of galactic chemical evolution, taking into account gaseous flows. We find that low-mass spirals must be several Gyr younger than massive ones. Also, we find that spirals with rotational velocities in the 80–400 km s^{-1} range must not have suffered extensive mass losses during their past history. Our conclusions are summarized in Section 6.

2 MODELLING THE EVOLUTION OF DISC GALAXIES

2.1 The model and the Milky Way

In Paper I, we presented a model for the chemical and spectrophotometric evolution of the Milky Way disc. We recall here the main ingredients of the model.

The disc is simulated as an ensemble of concentric, independently evolving rings, slowly built up by infall of primordial composition. For each ring we solve the classical equations of chemical evolution (e.g. Pagel 1997) without the assumption of the instantaneous recycling approximation (IRA). We use: stellar lifetimes from Schaller et al. (1992); the yields of Woosley & Weaver (1995) for massive stars, and those of Renzini & Voli (1981) for intermediate-mass stars; Type Ia supernovae (SNIa) producing Fe at a rate given in Matteucci & Greggio (1986); and the initial mass function (IMF) of Kroupa, Tout & Gilmore (1993) between 0.1 and 100 M$_\odot$. The adopted star formation rate (SFR) varies with gas surface density Σ_g and radius R as

$$\Psi(t,R) = \alpha \Sigma_g(t,R)^{1.5} V(R) R^{-1}, \quad (1)$$

where $V(R)$ is the rotational velocity, assumed to be 220 km s^{-1} in the largest part of the Milky Way disc. This radial dependence of the SFR is suggested by the theory of star formation induced by density waves in spiral galaxies (e.g. Wyse & Silk 1989). The efficiency α of the SFR (equation 1) is fixed by the requirement that the observed local gas fraction, at $R = 8$ kpc from the Galactic Centre ($\sigma_{gas} \sim 0.2$), is reproduced at $T = 13.5$ Gyr (our adopted value for the age of the local disc).

The disc is built up by infall at a rate exponentially decreasing in time, and a characteristic time-scale $\tau_{inf}(R)$ increasing with radius (so as to mimic the inside-out formation of the disc). The relation between $\tau_{inf}(R)$ and $\Sigma(R)$ (total surface density) is shown in Fig. 1 and is justified a posteriori, since it is crucial in shaping the various radial profiles (of gas, SFR, abundances, etc.) of the disc, which compare favourably to observations.

The spectrophotometric evolution is followed in a self-consistent way, with the metallicity-dependent stellar tracks from the Geneva group (Schaller et al. 1992; Charbonnel et al. 1996) and stellar spectra from Lejeune, Cuisinier & Buser (1997). Dust absorption is included according to the prescriptions of Guiderdoni et al. (1998) and assuming a 'sandwich' configuration for the stars and dust layers.

It turns out that the number of observables explained by the model is much larger than the number of free parameters. In particular, the model reproduces present-day 'global' properties (amounts of gas, stars, SFR and supernova rates), as well as the current disc luminosities in various wavelength bands and the corresponding radial profiles of gas, stars, SFR and metal abundances. Moreover, the adopted inside-out star-forming scheme leads to a scalelength of ~4 kpc in the B band and ~2.6 kpc in the K band, in agreement with observations (see Paper I).

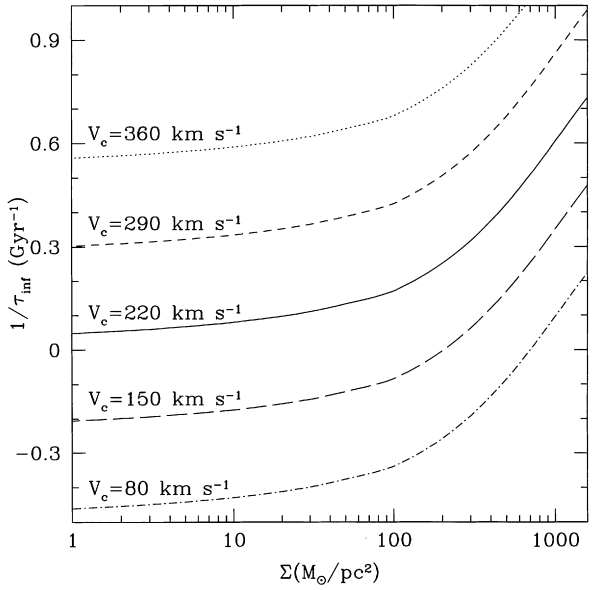

Figure 1. Infall time-scale τ_{inf} as a function of the local surface density Σ. The dependence on Σ is calibrated on the Milky Way (solid curve, $V_C = 220$ km s^{-1}). The dependence on V_C is chosen so as to reproduce the properties of the homogeneous sample of spiral galaxies presented in Section 3. When $\tau_{inf} < 0$, the infall is exponentially increasing with a time-scale $|\tau_{inf}|$.

2.2 Scaling relations

For a simplified extension of the model to the case of other disc galaxies, we adopt the 'scaling properties' derived by Mo, Mao & White (1998, hereafter MMW98) in the framework of the cold dark matter (CDM) scenario for galaxy formation. For the details, the reader should refer to MMW98 and Paper II. Discs form inside non-baryonic dark matter haloes of various masses and concentration factors. Assuming constant ratios of disc to halo mass (here taken to be $m_d = 0.05$), discs are characterized by two parameters: V_C, the circular velocity measuring the mass of the disc; and λ, the spin parameter measuring its angular momentum. A disc is described by its scalelength R_d and its central surface density Σ_0, which can be related to those of our Galaxy (designated by MW) by

$$\frac{R_d}{R_{d,MW}} = \frac{\lambda}{\lambda_{MW}} \frac{V_C}{V_{C,MW}} \quad (2)$$

and

$$\frac{\Sigma_0}{\Sigma_{0,MW}} = \left(\frac{\lambda}{\lambda_{MW}}\right)^{-2} \frac{V_C}{V_{C,MW}}. \quad (3)$$

The total mass of the disc M_d is proportional to V_C^3, but independent of λ. The λ distribution deduced from numerical simulations (see MMW98 and references therein) presents a maximum at $\lambda \sim 0.04$–0.05 and extends from ~0.01 to ~0.20. Since the value of λ_{MW} is not far from the peak value, we explored here values of λ in the range $\frac{1}{3}\lambda_{MW}$ to $3\lambda_{MW}$. Assuming that λ and V_C are independent, we constructed models with velocities in the

observed range 80 to 360 km s^{-1}. We calculated the velocity profile resulting from the disc plus an isothermal dark halo, and we used equation (1) to calculate self-consistently the SFR (with the same coefficient α, 'calibrated' on the Milky Way).

At this point it should be noted that our scaling relations (equations 2 and 3) are based on the assumption that angular momentum is conserved during the evolution of the disc. Numerical hydrodynamical simulations of galaxy formation (e.g. Navarro & Steinmetz 1999 and references therein) do not support this idea; indeed, it is found that, as the baryonic halo gas cools down and collapses to the disc, it loses most of its angular momentum. In those conditions, the final configuration of the disc cannot be related in a simple way to the initial λ of the halo. However, such simulations lead, in general, to disc sizes much smaller than observed. It is possible that star formation and feedback are not properly described in those simulations. For instance, Sommer-Larsen, Gelato & Vedel (1999) found that delaying the cooling of the gas reduces the loss of angular momentum. Since the situation is not clear yet, here we make the assumption of disc evolution at constant angular momentum, justified a posteriori by the fact that the resulting disc sizes are in agreement with observations (see Paper II). For a more detailed discussion of these issues, see also Cole et al. (2000).

2.3 Infall time-scales

The infall rate in our models is exponentially dependent on time, with a time-scale $\tau_{\rm inf}$ that depends on the surface mass density and is calibrated on the Milky Way disc (see Fig. 1); as explained in Paper II, we found that a dependence on the total mass of the galaxy is necessary in order to reproduce the observations of present-day discs. We consider that all the galaxies started forming their stars 13.5 Gyr ago and that the formation of their exponential discs (characterized by Σ_0 and $R_{\rm d}$) was completed at the present epoch. Notice that the value of $T = 13.5$ Gyr plays no essential role in the results of this work (values in the 10–15 Gyr range would lead to quite similar conclusions); these results depend mainly on the infall time-scales. The more massive galaxies are characterized by shorter formation time-scales, while less massive galaxies are formed on longer ones (Fig. 1). This assumption turned out to be a crucial ingredient of our models, allowing us to reproduce an impressive amount of observed properties of spirals that depend on mass (or $V_{\rm C}$): colours, gas fractions, abundances and integrated spectra. Those observables are thoroughly presented in Paper II, while some of them are revisited in this work. In Paper III, we show that this model also reproduces fairly well the observed colour and abundance gradients in spirals.

We notice that Bell & de Jong (2000) suggested recently that the observed colour gradients of disc galaxies correlate very well with the local surface density, in the sense that inner and denser regions are older. Our assumption about the infall time-scale agrees, at least qualitatively, with their findings.

We stress that infall time-scales are *inputs* to the model, and adjusted so as to reproduce observations. Star formation time-scales are *outputs* of the model (resulting from the adopted prescriptions for infall *and* SFR) and are presented in Section 4.1.

3 COMPARISON WITH OBSERVATIONS

3.1 The observational sample

The sample of galaxies analysed in this work, which has been extracted from the large multifrequency data base of nearby galaxies of Gavazzi & Boselli (1996), is extensively described in Boselli et al. (2001). Here we give just a brief description of the sample selection criteria: we refer the reader to Boselli et al. (2000) for detailed references on the data and on their analysis.

Galaxies analysed in this work are taken from the Zwicky catalogue (CGCG; Zwicky et al. 1961–68) ($m_{\rm pg} \leqslant 15.7$). They are either late-type (type $>$ S0a) members of three nearby (recession velocity $cz \leqslant 8000$ km s^{-1}) clusters (Cancer, A1367, Coma), or located in the relatively low-density regions of the Coma–A1367 supercluster ($11^{\rm h}30^{\rm m} < {\rm RA} < 13^{\rm h}30^{\rm m}$, $18° < {\rm Dec.} < 32°$) as defined in Gavazzi, Carrasco & Galli (1999a). To extend the present study to lower luminosities, we include in the sample the late-type Virgo cluster galaxies brighter than $m_{\rm pg} \leqslant 14.0$ listed in the Virgo Cluster Catalogue (VCC; Binggeli, Sandage & Tammann 1985) as cluster members. Furthermore VCC galaxies with $14.0 \leqslant m_{\rm pg} \leqslant 16.0$ included in the 'ISO' subsample described in Boselli et al. (1997a) and CGCG galaxies in the region $12^{\rm h} < {\rm RA} < 13^{\rm h}$, $0° < {\rm Dec.} < 18°$ but outside the VCC are considered.

To avoid systematic environmental effects, we consider the subsample of late-type galaxies whose H I deficiency [defined as $d = \log({\rm H\,I}/\langle {\rm H\,I}\rangle)$, the ratio of the H I mass to the average H I mass in isolated objects of similar morphological type and linear size (see Haynes & Giovanelli 1984)] is $d \geqslant 0.3$, typical of unperturbed, isolated galaxies. The final combined sample comprises 233, mainly 'normal' galaxies.

We assume a distance of 17 Mpc for the members (and possible members) of Virgo cluster A, 22 Mpc for Virgo cluster B, and 32 Mpc for objects in the M and W clouds (see Gavazzi et al. 1999b). Members of the Cancer, Coma and A1367 clusters are assumed to be at distances of 62.6, 86.6 and 92 Mpc respectively. Isolated galaxies in the Coma supercluster are assumed at their redshift distance adopting $H_0 = 75$ km s^{-1} Mpc^{-1}.

For the 233 optically selected galaxies, data are available in several bands as follows: 100 per cent have H I (1420 MHz) and 99 per cent H-band (1.65 μm) data, while a much coarser coverage exists in the UV (2000 Å) (29 per cent), CO (115 GHz) (38 per cent) and Hα (6563 Å) (65 per cent), as shown in tables 1 and 2 of Boselli et al. (2001). The distribution of the sample galaxies in the different morphological classes is given in table 3 of Boselli et al. (2001).

As previously discussed, the present sample is optically selected and thus can be biased against low surface brightness galaxies; the inclusion of the Virgo cluster should in principle favour the presence of some low surface brightness galaxies, not easily detectable at higher distances. Being volume limited, the sample is not biased towards bright, giant spirals, but it includes also dwarfs and compact sources. Its completeness at different wavelengths makes this a unique sample suitable for statistical analysis.

3.2 Data analysis

Hα and UV fluxes, corrected for extinction (and [N II] contamination) as described in Boselli et al. (2001), are used to estimate star formation rates through population synthesis models given in that work; a power-law IMF of slope -2.5 with a lower and upper mass cut-off of 0.1 and 80 M$_\odot$, respectively, is adopted. Its high-mass part is quite similar to that of the IMF of Kroupa et al. (1993), adopted in our models. Given the uncertainty in the UV and Hα flux determination, in the extinction correction and in the transformation of the corrected fluxes into SFRs via

population synthesis models, we estimate an uncertainty of a factor of ∼3 in the determination of the SFR.

The total gas content of the target galaxies, H I + H_2, has been determined from H I and CO measurements. CO (at 2.6 mm) fluxes have been transformed into H_2 masses assuming a standard CO to H_2 conversion factor of 1.0×10^{20} mol cm^{-2} (K km s^{-1})$^{-1}$ (Digel et al. 1996). For galaxies with no CO measurement, we assume that the molecular hydrogen content is 10 per cent of the H I, as estimated from isolated spiral galaxies by Boselli et al. (1997b). The total gas mass has been corrected for He contribution by 30 per cent. H I fluxes are transformed into neutral hydrogen masses with an uncertainty of ∼10 per cent. The average error on CO fluxes is ∼20 per cent; the error on the H_2 content, however, is significantly larger (and difficult to quantify) because of the poorly known CO to H_2 conversion factor (see Boselli et al. 1997b).

Galaxy colours have been determined from broad-band near-IR and optical photometry. Near-IR (*H*-band) images are available for 230 of the 233 sample galaxies, while *B* images or aperture photometry are available for 214 objects. The *H* and *B* magnitudes have been corrected for extinction as in Gavazzi & Boselli (1996). No correction has been applied to galaxies of type later than Scd. The estimated error on *B* and *H* magnitudes is 15 per cent.

Rotational velocities have been determined from the H I linewidth at 21 cm, and corrected for inclination as in Gavazzi (1987). To avoid large systematic errors, we estimate rotational velocities only for galaxies with inclinations >30° and with the 21-cm linewidth accurately determined (double- or single-horned profile with high signal-to-noise ratio). The uncertainty on the determination of the rotational velocity is ∼15 km s^{-1}.

In summary, we have a homogeneous sample of 233 normal (non-perturbed) disc galaxies. For 96 of them, we evaluated all the quantities of interest in this work: blue magnitude M_B, total mass M_T, total gas mass M_g, star formation rate Ψ and rotational velocity V_C. We shall see below how our models fit those properties and what kind of inferences can be made on the star formation history of those galaxies.

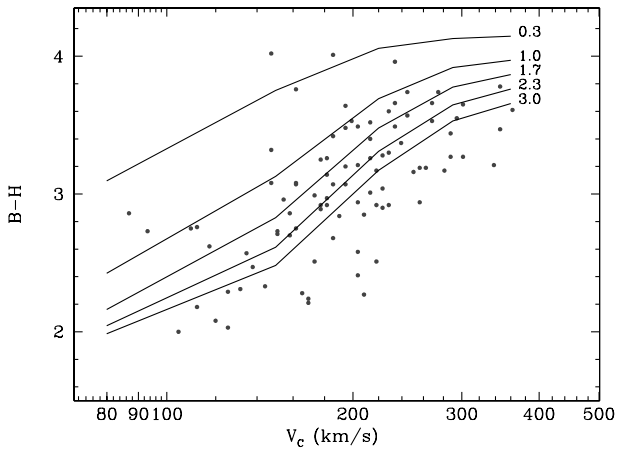

Figure 2. Colour index $B - H$ versus rotational velocity V_C. Symbols are observations presented in Section 3.1. A clear correlation is obtained, with massive discs being redder than low-mass ones. The curves are the results of our models and are labelled by the value of the ratio λ/λ_{MW}, where λ_{MW} is the spin parameter for the Milky Way disc. The upper curve corresponds to very low values of λ, producing very compact galaxies that look like bulges or ellipticals rather than spirals.

3.3 Mass-driven colours and gas fractions

In Fig. 2 we compare our model results with the colours $B - H$ of our galaxy sample. A clear correlation is obtained between $B - H$ and V_C, with the more massive discs being, on average, redder than their lower-mass counterparts. Our models (solid curves) reproduce naturally the observed correlation, since *by construction* the more massive discs form their stars earlier (Fig. 1). The corresponding time-scales for star formation will be discussed in Section 4.1. The observed dispersion in the lower panel of Fig. 2 can be accounted for by the range of λ values in our models, but only partially. Discs with lower λ are more compact, have higher central surface densities and evolve earlier than those with larger λ. Obviously, λ values larger than $3\lambda_{MW}$ (the largest value used here) would lead to even smaller $B - H$ values than the models displayed on Fig. 2, possibly accounting for the rest of the scatter.

We notice that our models do take extinction by dust into account (with the prescriptions presented in Section 2.1), and that extinction contributes somewhat (by ∼0.5 mag) in reddening the most massive discs in our models, which have relatively large amounts of metals. However, we insist on the fact that it is *age*, not extinction, that is mainly responsible for the trends of our models in Fig. 2.

In Fig. 3 we present two important pieces of data, on which the main argument of this paper is based. In the upper panel, we show the ratio M_g/L_H (mass of gas to *H*-band luminosity) versus

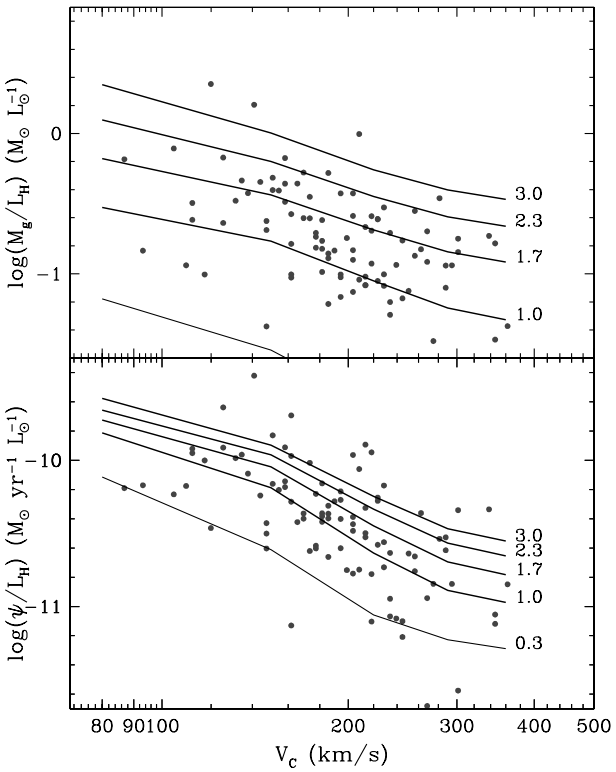

Figure 3. Upper panel: Ratio M_g/L_H of gas mass to *H*-band luminosity versus rotational velocity V_C; this is a measure of gas fraction. Lower panel: Ratio Ψ/L_H of star formation rate to *H*-band luminosity versus rotational velocity V_C; this is a measure of the present SFR compared to the past average one. Massive discs have smaller gas fractions and were more active in the past than their lower-mass counterparts. In both panels, our models (parametrized with the spin parameter λ/λ_{MW}, where λ_{MW} is the Milky Way value of λ) are in fair agreement with the data.

rotational velocity V_C. Since L_H reflects the mass of the stellar population (Gavazzi et al. 1996), this ratio is a measure of the gas fraction of the system. Despite the large scatter, it is clear that a correlation does exist, the more massive galaxies being, in general, gas-poor. Our model results can fairly well describe the observations, accounting for both the slope and the dispersion of the M_g/L_H versus V_C relation.

In the lower panel of Fig. 3 we plot the ratio Ψ/L_H (current SFR to H-band luminosity) versus V_C. As discussed in several places (e.g. Kennicutt 1998a), this ratio is a measure of the parameter $b = \Psi/\langle\Psi\rangle$, the ratio of the current SFR to the past average one. Massive galaxies display smaller Ψ/L_H, and thus lower b values, than their low-mass counterparts. This means that they formed their stars at much higher rates in the past. Again, our results compare fairly well with the data, concerning both the slope and the scatter of the correlation. For a given V_C, large λ discs have larger gas fractions today and were less active in the past than their lower λ counterparts. As we shall see in Section 4.3, and discuss in Section 5, when the two panels of Fig. 3 are combined, they suggest quite convincingly that low-mass spirals are on average younger than massive ones.

At this point, we notice that Gavazzi & Scodeggio (1996) have already advanced a similar hypothesis to explain the observed colours of galaxies as a function of their H-band luminosity (a measure of their dynamical mass according to them). Gavazzi et al. (1996) came to similar conclusions and suggested that mass is the main parameter of galaxy evolution, on the basis of multiwavelength observations concerning a variety of disc properties (colours, gas content, star formation rate, radius, surface brightness).

4 STAR FORMATION HISTORIES IN DISCS

4.1 Formation time-scales

The Hubble sequence of galaxies is usually interpreted in terms of different star formation time-scales (e.g. Kennicutt 1998a), although such an interpretation leaves unclear the role of the mass of the galaxy (Prantzos 2000). In order to put our results in that context, we performed an exponential fit to the star formation histories of our model galaxies (excluding the first 2 Gyr, where such a fit turns out to be inadequate). The resulting time-scales are shown in Fig. 4. Notice that in some models the SFR is continuously increasing with time, resulting in negative characteristic time-scales. For that reason we present τ_{EXP}^{-1}, which has the advantage of varying continuously when going from an SFR increasing with time to one decreasing with time. For an exponential star formation rate, $\Psi \propto \exp(-t/\tau_{EXP})$, τ_{EXP}^{-1} is equal to $-\dot{\Psi}/\Psi$ (where $\dot{\Psi} = d\Psi/dt$) and can be considered as the normalized rate of change of the SFR. Obviously, the larger τ_{EXP}^{-1}, the earlier the galaxy forms its stars.

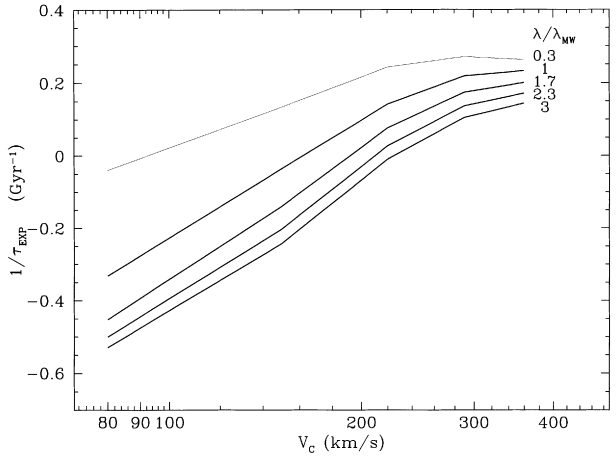

Figure 4. Time-scale of an exponential fit to the star formation rate history of our model galaxies; τ_{EXP}^{-1} (Gyr^{-1}) is plotted as a function of disc rotational velocity V_C and parametrized with the spin parameter λ/λ_{MW}. For low values of V_C, τ_{EXP} is negative, i.e. the star formation rate is increasing with time. τ_{EXP}^{-1} is larger for massive galaxies, which form their stars earlier.

As can be seen on Fig. 4, massive galaxies in our models form their stars on shorter time-scales than their lower-mass counterparts. This general trend is somewhat modulated by the spin parameter λ: discs with smaller λ (i.e. more compact) have larger τ_{EXP}^{-1} than discs with larger λ of similar rotational velocity. The most massive discs of our simulations ($V_C = 360\,km\,s^{-1}$) have decreasing SFR with $\tau_{EXP} \sim 4$–5 Gyr. Discs with $V_C \sim 200\,km\,s^{-1}$ have long time-scales, of the order of $\sim$10 Gyr, i.e. essentially constant SFR. Finally, low-mass discs ($V_C \sim 100\,km\,s^{-1}$) have SFR increasing in time, with characteristic time-scales $\tau_{EXP}^{-1} \sim -0.2$ to $-0.5\,Gyr^{-1}$.

4.2 The evolution of the star formation efficiency

What is the reason for the vastly different SF time-scales obtained in our models as a function of V_C? Is the overall SF efficiency $\epsilon = \Psi/M_g$ directly affected by the mass of the galaxy? An inspection of equation (1) suggests that this cannot be the reason. Indeed, at the characteristic radius of the disc R_d, the local efficiency is

$$\epsilon(R_d) = \Psi(R_d)/\Sigma_g(R_d) = \alpha\Sigma_g^{0.5} V R_d^{-1} \propto \lambda^{-2} V^{0.5}, \quad (4)$$

since $R_d \propto \lambda V$ from equation (2) and $\Sigma(R_d) \propto \Sigma_0 \propto \lambda^{-2} V$ from equation (3). In other terms, the SF efficiency at R_d varies very

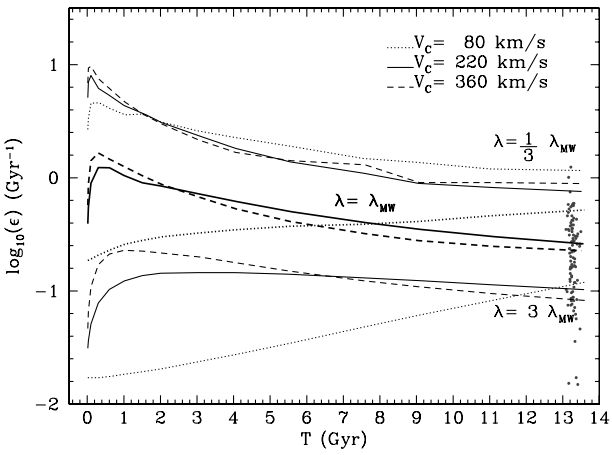

Figure 5. Evolution of the star formation efficiency ϵ (Ψ/M_g) as a function of time for three families of models labelled by their λ values ($\frac{1}{3}$, 1 and $3 \times \lambda_{MW}$). Low λ values correspond to more compact galaxies, while values larger than $3\lambda_{MW}$ lead to low surface brightness galaxies. For each λ, three curves are shown corresponding to $V_C = 80$, 220 and 360 km s^{-1}, respectively. The SF efficiency ϵ depends more on λ than on V_C. At $T = 13.5$ Gyr, the present-day observations (Section 4.3) are shown; an artificial small age spread is introduced. Our grid of models at $T = 13.5$ Gyr covers well the observed ϵ values.

little with V_C and depends much more on λ than on V_C. Since the value of any intensive quantity (like SF efficiency) at R_d is typical of the whole disc, it is expected that the global SF efficiency also depends little on V_C. In order to show this quantitatively, we plot in Fig. 5 the evolution of the global SF efficiency ϵ of our models as a function of time. We show the results for three values of λ ($\frac{1}{3}$, 1 and $3\times\lambda_{MW}$) and three values of V_C (80, 220 and 360 km s^{-1}, respectively). We compare our results at $T = 13.5$ Gyr to estimates of $\epsilon = \Psi/M_g$ in our sample of nearby spirals (presented in Section 4.3). The following points should be noted concerning our models:

(i) The efficiency ϵ depends very little on V_C, especially during the last half of the history of the galaxy.

(ii) The efficiency ϵ is mainly determined by λ: 'compact' galaxies have higher efficiency because of their smaller size ($\Psi \propto 1/R$, for a given V_C) and larger gas surface density at the characteristic radius R_d. At $T = 13.5$ Gyr, the variation of our ϵ values due to λ can fully account for the dispersion in ϵ measured in nearby spirals.

(iii) The SF efficiency in compact galaxies (low λ) presents a peak at early times and then decreases. This happens because the star formation migrates to outer regions (because of the inside-out disc formation scheme) where the local SF efficiency is lower (because of lower surface densities and the $1/R$ factor). In more extended galaxies (larger λ), ϵ does not present such a decrease because local properties vary little with radius.

(iv) For the lowest disc velocities V_C, ϵ may increase with time. This is due to the adopted form of infall: the gas surface density increases considerably when the gas arrives finally in the disc (which may take a very long time in the case of the largest λ values and lowest V_C values; see Fig. 4).

The main point of this section is that in our models the SF efficiency ϵ does not depend directly on the mass of the galaxy. The range of ϵ spanned by our models during galactic evolution is due to λ and τ_{inf}, not to V_C; the most important of the two parameters is τ_{inf}. Of course, τ_{inf} is adjusted to V_C, so that the observations of Figs 2 and 3 (and many others, presented in Paper II) are reproduced. This is a crucial ingredient for the success of our models, and we discuss its implications in Section 5.

4.3 Gas fraction and star formation efficiency

The analysis of Sections 4.1 and 4.2 leads to an important conclusion: the success of our models is to be interpreted in terms of mass-dependent SF time-scales. But this is not due to any explicit dependence of SF *efficiency* on galaxy mass. Indeed, the SF efficiency of our models is virtually independent of mass during most of galactic history, and in particular at the present time. Is this supported by observations?

In Fig. 6 we display our data of Fig. 3, this time in a more 'physical' presentation, appropriate for a quantitative discussion (see Section 5). The gas fractions σ_{gas} (upper panels) and SF efficiency ϵ (lower panels) are presented as a function of

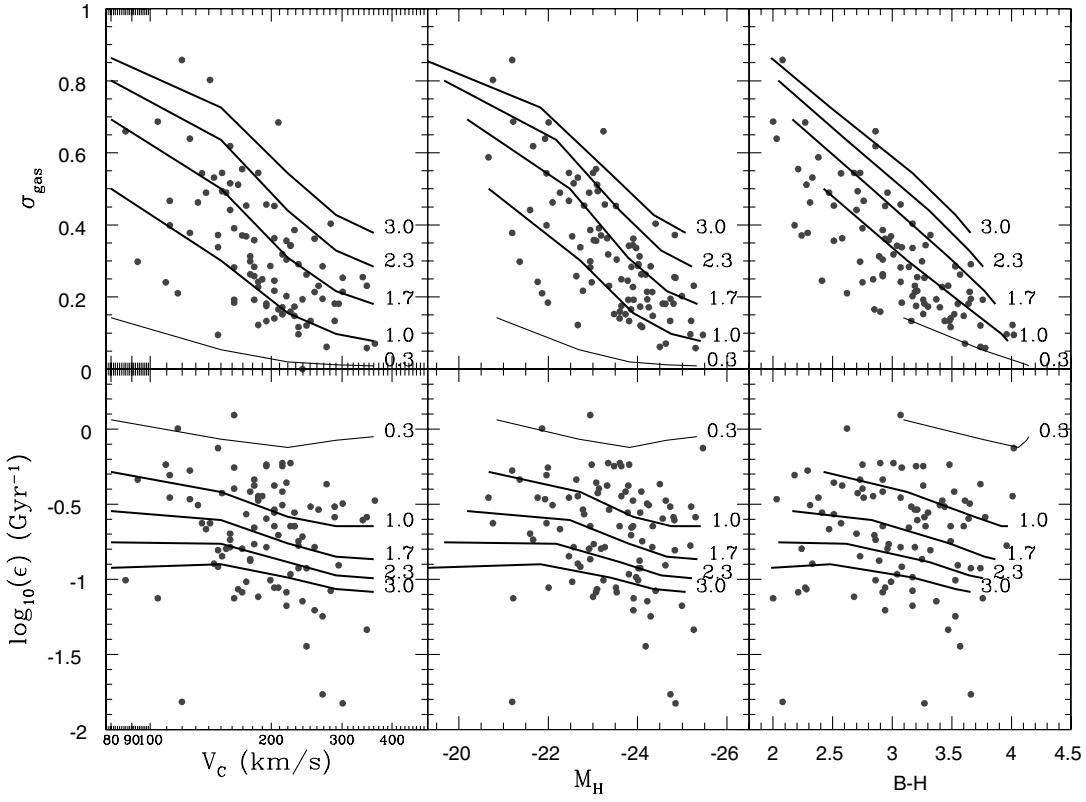

Figure 6. Gas fraction ($\sigma_{gas} = M_g/M_T$, upper panels) and global star formation efficiency ($\epsilon = \Psi/M_g$, lower panels) versus circular velocity V_C (left panels), H-band magnitude (middle panels) and colour index $B - H$ (right panels). Dots represent our data (Section 4.3). The results of our models (Section 4.2) are shown by curves, parametrized by the ratio λ/λ_{MW}, where λ_{MW} is the Milky Way spin parameter. The gas fraction decreases, on average, with galaxy mass, luminosity and colour index, while the global SF efficiency ϵ does not depend on those parameters. Our models account fairly well for these data. We note that ϵ_{model} is a function of λ and is greater for compact galaxies.

rotational velocity V_C (left panels), H magnitude (middle panels) and $B-H$ colour (right panels).

The gas fraction $\sigma_{gas} = M_g/M_T$ (where the total mass $M_T = M_* + M_g$ is the mass of stars + gas) is obtained by converting the L_H luminosity to star mass M_* through the mass-to-light ratio M_*/L_H obtained in our models. This value is in the 0.3–0.6 range in solar units ($M_*/L_H \sim 0.35$ for $V_C = 80\,km\,s^{-1}$, $\sim$0.47 for $V_C = 220\,km\,s^{-1}$ and $\sim$0.56 for $V_C = 360\,km\,s^{-1}$). Despite the uncertainties, a clear trend is present in the upper panel: the more massive, luminous and red a galaxy is, the smaller is its gas fraction. Notice that a similar trend is obtained by McGaugh & de Blok (1997) and Bell & de Jong (2000). Our model results are in excellent agreement with the data, although we have some difficulty in reproducing blue and gas-poor discs (with $B - H < 2.5$ and $\sigma_{gas} < 0.4$).

The SF efficiency of our observed galaxies is obtained by simply dividing the SFR Ψ by the gas mass M_g. We notice that the uncertainties in deriving ϵ are rather large: those concerning the SFR Ψ are quite large (a factor of $\sim$3), whereas those of the gas mass are at least of $\pm$20 per cent. As a result, the observationally derived scatter of ϵ, as appears on Figs 5 and 6, is certainly larger that the real one. It is clear, however, that the SF efficiency does not seem to be correlated with the mass or the colours of spirals. The scatter in the observed values of ϵ (a factor of $\sim$10) should be compared to the range of $\sim$60 spanned by galaxy mass (since the mass of the disc $m_d \propto V_C^3$) or the range of five magnitudes in H luminosity. Our model SF efficiencies ϵ at $T = 13.5\,Gyr$, also displayed in Fig. 6 (lower panel, solid curves), show no dependence on mass or colour. They also reproduce the observed dispersion, the more compact discs (smaller λ) being the more efficient in turning their gas into stars.

The upper and lower panels of Fig. 6, when combined, point to an important conclusion: since the SF efficiency is independent of galactic mass (or luminosity), the fact that low-mass galaxies have larger gas fractions today may only be the result of their smaller ages. This is the most straightforward interpretation, independent of any theoretical considerations (except for the implicit assumption that the SF efficiency has remained approximately constant during the history of the galaxy). This conclusion is corroborated by an independent observable, namely that low-mass galaxies are, in general, bluer than more massive ones. Notice that the latter observable concerns also elliptical galaxies, but the well-known problem of the age–metallicity degeneracy does not allow one to make conclusions in that case. In the case of spirals, the situation is even worse in principle, because colours may be affected by the presence of dust (presumably more abundant in massive spirals). Because of this complication, the observed gas fraction (smaller in large spirals) is not sufficient in itself to lift the age–metallicity degeneracy. However, when combined with the fact that the SF efficiency is independent of galactic mass (as argued here), the degeneracy is lifted, and the aforementioned conclusion is naturally obtained.

Before turning to a more detailed discussion of our findings, we would like to point out that similar results are obtained in other recent works. For instance, McGaugh & de Blok (1997) find a clear trend between the gas fraction and the B magnitude of their galaxy sample, which they describe by the relation $\sigma_{gas} = 0.12(M_B + 23)$. This relationship is shown in Fig. 7 (upper panel, dashed line), along with the McGaugh & de Blok (1997) data for normal spirals and our data for normal spirals. It can be seen that there is a very good agreement between the two data sets.

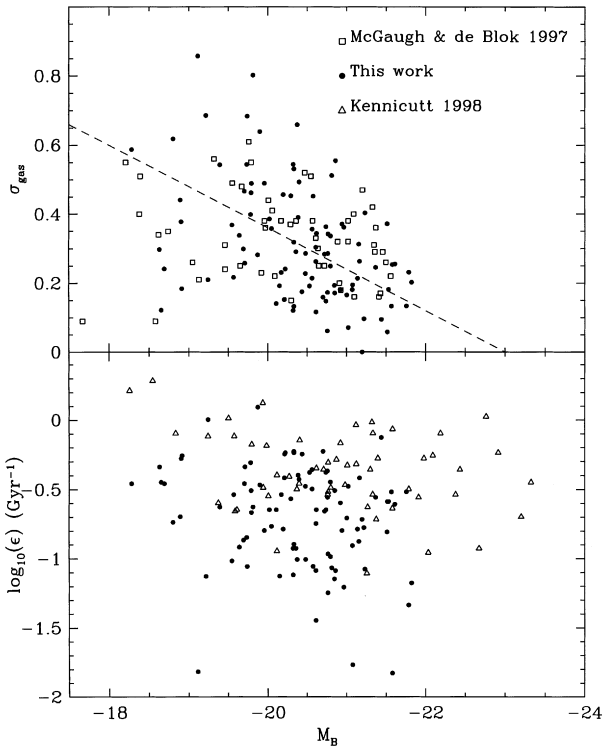

Figure 7. Gas fraction ($\sigma_{gas} = M_g/M_T$, upper panels) and global star formation efficiency ($\epsilon = \Psi/M_g$, lower panels) versus B-band magnitude. Our data are shown by filled symbols in both panels. They are in agreement with data from other surveys: McGaugh & de Blok (1997), squares in the upper panel; and Kennicutt (1998b), triangles in the lower panel. The same trends as in Fig. 6 are also obtained here (i.e. gas fraction decreasing with galaxy luminosity, and star formation efficiency independent of luminosity). The dashed curve in the upper panel is a fit to the McGaugh & de Blok (1997) data: $\sigma_{gas} = 0.12(M_B + 23)$.

We notice that our models fit the observations of McGaugh & de Blok (1997) fairly well (see fig. 13 of Paper II).

In the lower panel of Fig. 7 we show the SF efficiency, both for our data set and for that of Kennicutt (1998b). Notice that Kennicutt (1998b) gives the *average* SFR surface density $\langle\Psi\rangle$ and *average* gas surface density $\langle\Sigma_{gas}\rangle$ of normal spirals, i.e. the integrated quantities are divided by the disc surface area (within the optical radius). Obviously, the ratio $\langle\Psi\rangle/\langle\Sigma_{gas}\rangle$ gives the overall SF efficiency ϵ (since the disc area cancels out). As can be seen in Fig. 7, Kennicutt's values of the SF efficiency are slightly larger than ours (by a factor of $\sim$2), and have a smaller dispersion in the adopted logarithmic scale. Taking into account the various uncertainties in estimating the SFR from the data (see Section 3), such a discrepancy between Kennicutt's results and ours is not unexpected. But the important point is that Kennicutt's values are also independent of the galaxy B luminosity and, by virtue of the Tully–Fisher relation, of the mass of the galaxy.

The anticorrelation between gas fraction and luminosity in spirals was noticed by several authors (e.g.Gavazzi et al. 1996; McGaugh & de Blok 1997; Bell & de Jong 2000; Boselli et al. 2000). Based on two independent samples, we showed here that the SF efficiency of spirals is independent of their mass. The two findings combined point to small discs being younger, on average, than massive ones. Our model, presented in Section 3.2, nicely explains these features (and several others, presented in Papers II and III). However, one may argue that the complex

interdependence between the adopted infall and SFR prescriptions makes a straightforward interpretation difficult; one may also argue that other types of models could also account for the observations and give a different interpretation for the same data (e.g. by invoking outflows). For that reason, in the next section we discuss this issue on the basis of simple analytical models of galactic chemical evolution, and we make a very rough evaluation of the 'ages' of the galaxies in our sample. Our purpose is not to derive the exact ages of the galaxies, but rather to have an order-of-magnitude estimate and, in particular, to check whether there is any *trend* of the derived ages with galactic mass.

5 GALACTIC AGES

In the framework of simple models of galactic chemical evolution adopting the instantaneous recycling approximation (IRA), one may obtain analytical solution for various quantities. In particular, provided that the star formation rate Ψ is proportional to the gas mass $M_{\rm g}$, i.e.

$$\Psi = \epsilon M_{\rm g}, \tag{5}$$

one may obtain a relationship between the gas fraction $\sigma_{\rm gas}$ and time T (assuming that the SF efficiency ϵ is constant in time). The form of this relationship depends on further assumptions about the evolution of the system, i.e. on the possibility of allowing for gas flows inside or outside the 'box' (e.g. Pagel 1997).

Assuming that the galaxies of our sample have evolved as simple, homogeneous, 'boxes', we consider three possibilities: a 'closed box' (all the gas is present from the very beginning), an 'infall' model (where gas mass is continuously added to the system), and an 'outflow' model (with gas continuously leaving the system). In the cases of gaseous flows, further assumptions about the corresponding flow rates are required in order to obtain analytical solutions. More specifically:

(a) *Closed box*. In that case, we have

$$\sigma_{\rm gas} = \exp[-(1-R)\epsilon T], \tag{6}$$

where the return fraction R accounts for the gas returned by stars to the interstellar medium; for the IMF of Kroupa et al. (1993) adopted here we have $R \sim 0.32$.

(b) *Infall*. An analytical solution is easily obtained if it is assumed that the infall rate just balances the gas depletion due to star formation. As we have shown in Paper II, with detailed numerical models reproducing a large body of observational data, this situation describes rather well the largest period in the lifetime of most spiral galaxies. In that case, we have

$$\sigma_{\rm gas} = [1 + \epsilon(1-R)T]^{-1}. \tag{7}$$

(c) *Outflow*. Analytical solutions may be obtained by assuming that the outflow rate is proportional to the SFR, $f_{\rm out} = \gamma\Psi$. In that case, we have

$$\sigma_{\rm gas} = \frac{R-1-\gamma}{(R-1)\exp[-\epsilon(R-1-\gamma)T] - \gamma}. \tag{8}$$

We shall assume here that the outflow rate is equal to the SFR, i.e. $\gamma = 1$ (since, for higher outflow rates, we obtain ridiculously low galactic ages).

For each of the three scenarios, we shall consider five combinations between the observed gas fraction and SF efficiency, in order to derive galactic age T through equations (6), (7) and (8). For the gas fraction versus rotational velocity, we adopt the three curves of the upper panel of Fig. 8, corresponding roughly to the mean trend and the upper and lower bounds of the observations, respectively. For each of those three curves, we derive the corresponding galactic ages by using an SF efficiency $\epsilon = 0.3\,{\rm Gyr}^{-1}$ (the mean value of the observations in Figs 6 and 7). In that way, we obtain the shaded regions in Fig. 8, with the thick curve corresponding to the mean trend, the largest ages to the lowest gas fractions and vice versa. We perform two more calculations. For the first, we adopt the high gas fractions (uppermost curve in the upper panel of Fig. 8), combined with a low SF efficiency $\epsilon = 0.1\,{\rm Gyr}^{-1}$ (a reasonable lower bound for the observations of Figs 6 and 7). In that way we obtain the dotted curves in Fig. 8. Finally, we adopt the low gas fractions (lower curve in the upper panel of Fig. 8), combined with a high SF efficiency $\epsilon = 1\,{\rm Gyr}^{-1}$

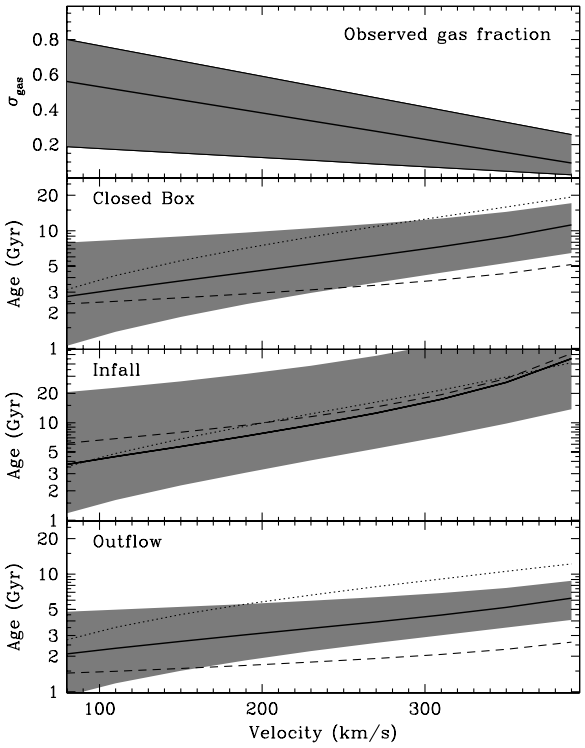

Figure 8. Upper panel: Observed gas fraction versus galaxy rotational velocity. The three curves represent, schematically, the mean trend (thick curve), and the upper and lower bounds of the observed gas fractions in Fig. 6. Given the star formation efficiency ϵ, the shaded area inside the upper and lower curves may be used to derive approximate ages for the galaxies, in the framework of simple analytical models for galactic chemical evolution, using the IRA. This is done in the next three panels: for a closed box, a model with infall (such that the gas mass remains constant in time) and a model with outflow (with an outflow rate equal to the star formation rate). In each of those panels, the thick curve corresponds to the mean gas fraction of the upper panel and a SF efficiency $\epsilon = 0.3\,{\rm Gyr}^{-1}$ (the mean value for the efficiencies in Fig. 6). The shaded area is obtained by keeping the same SF efficiency, but considering the upper and lower bounds for the observed gas fraction in the upper panel (lower gas fractions lead to larger ages for a given rotational velocity). The dotted curves are obtained with the low gas fractions combined with a high SF efficiency ($\epsilon = 1\,{\rm Gyr}^{-1}$, a reasonable upper bound for the observed ϵ values in Fig. 6). Finally, the dashed curves are obtained with the high gas fractions combined with a low SF efficiency ($\epsilon = 0.1\,{\rm Gyr}^{-1}$, a reasonable lower bound for the observed ϵ values in Fig. 6).

(a reasonable upper bound for the observations of Figs 6 and 7). In that way we obtain the dashed curves in Fig. 8.

An inspection of the results, plotted in the three lower panels of Fig. 8, shows that the derived 'effective' galactic age is a monotonic function of rotational velocity V_C in all cases. The absolute ages depend, of course, on the adopted gas fractions, SF efficiencies and assumptions about gaseous flows. For a given gas fraction and SF efficiency, the infall model leads to the largest ages; since the gas is constantly replenished, it takes more time to attain a given gas fraction than in a closed box (starting with $\sigma_{gas} = 1$). Also, the outflow model produces the lowest ages; since part of the gas is constantly removed, it takes less time to reach a given gas fraction than in a closed box. The ages derived in the framework of the outflow model are, in general, too low: they are lower than 6 Gyr for all galaxies with $V_C < 200\,km\,s^{-1}$. It transpires that galaxies in this velocity range should not have suffered extensive mass losses, i.e. they must not have lost during their lifetime an amount of gas as important as their stellar content (since we adopted $f_{out} = \Psi$ here).

The mean age values in the case of the infall model are 4–5 Gyr for the small discs (in the $V_C \sim 100\,km\,s^{-1}$ range) and ~10 Gyr for $V_C \sim 220\,km\,s^{-1}$. For discs with $V_C > 300\,km\,s^{-1}$, extremely large ages (>15 Gyr) are found; however, the approximation of evolution at constant gas mass is certainly not valid in that case (see fig. 4 in Paper II). We note that Bell & de Jong (2000), on the basis of a different sample and with a completely different method (based on a photometric estimate of the ages), find an 'effective age' of ~10 Gyr for the more luminous galaxies ($M_K \sim -26$) and ~6 Gyr for the less luminous ones ($M_K \sim -20$); the galaxies of our sample also span this luminosity range, and it is interesting to see that similar ages are found with completely independent methods.

The results obtained in this section confirm the suggestion of Section 3.2: low-mass discs are, on average, younger than massive ones. The only way to reverse this trend is by assuming that the SF efficiency is strongly correlated with disc mass. Despite the large scatter in the observational data, it is clear that such a correlation does not exist, at least at the present time; and, since the observed galaxies span a large range in masses and metallicities, it does not seem plausible that such a correlation ever existed in the past. In the case of outflow models, another possibility would be to consider that the more massive discs suffered more important mass losses (leading to low gas fractions without having to invoke large ages). However, such a hypothesis is incompatible with the fact that massive discs have deeper potential wells and are less prone to outflows than low-mass ones.

6 SUMMARY

In this work we investigate the properties of the star formation efficiency of spiral galaxies and study the implications for their evolution. We use a large homogeneous sample of disc galaxies, for which we measure gaseous mass M_g (H I), rotational velocity V_C, star formation rates Ψ and luminosities in the B and H bands. We are then able to derive the corresponding gas fractions σ_{gas} and SF efficiencies $\epsilon = \Psi/M_g$ as a function of V_C, H luminosity and $B-H$ colour index. We find that the gas fraction is correlated to V_C, H luminosity and $B-H$, in the sense that more massive, luminous and redder discs have smaller gas fractions. Previous work by McGaugh & de Blok (1997) reached similar conclusions. The main finding of this work is that the SF efficiency does not correlate with any of the galaxy properties; despite a rather large dispersion (within a factor of ~10), the observed ϵ is independent of V_C, L_H or $B-H$.

We interpret our data in the framework of detailed models of galactic chemical and spectrophotometric evolution, utilizing metallicity-dependent stellar lifetimes, yields, tracks and spectra. These models are calibrated on the Milky Way disc (Paper I) and use radially dependent star formation rates, which reproduce observed gradients (Paper III). They are extended to other spirals in the framework of cold dark matter scenarios for galaxy formation, and are described by two parameters: rotational velocity V_C and spin parameter λ. As in our previous work (Paper II), we find good agreement with the observations, provided a crucial assumption is made: massive discs are formed earlier than less massive ones. With this assumption our models reproduce the observed trends of gas fractions and SF efficiencies versus V_C, while variations due to λ account for the observed dispersion in both cases.

It is important to notice that the dependence of age on galactic mass that we find is not due to any mass-dependent SF efficiency, only to disc formation time-scales; in our models this is achieved by varying the infall time-scales. Both observations and models suggest that the SF efficiency is independent of galaxy properties. Since the observed galaxies cover a wide range of masses, colours and metallicities, there is no reason to suppose that the SF efficiency was different in the past. The adopted SFR prescription in our models also results in a very slowly varying SF efficiency with time.

When the observed relations of gas fraction versus V_C and SF efficiency versus V_C are considered in combination, they convincingly suggest that low-mass discs are, on average, younger than more massive ones; this conclusion is independent of any model and the only assumption is that the SF efficiency is constant in time (a quite plausible assumption, as argued above). In the framework of simple analytical models of galactic chemical evolution, we evaluate the 'effective ages' for the galaxies of our sample, using the observationally derived values of σ_{gas} and ϵ. We find that even models with modest outflows (with ejected masses equal to the stellar ones) lead to ridiculously low values for the galaxy ages; our conclusion is that galaxies in the range $V_C \sim 80$–$400\,km\,s^{-1}$ have not suffered extensive mass losses. Closed box models and infall models lead to more plausible values for the effective ages. In particular, infall models lead to ages of ~4–5 Gyr for discs of $V_C \sim 100\,km\,s^{-1}$ and ~8–10 Gyr for $V_C \sim 200\,km\,s^{-1}$. These 'chemically derived' ages are in fair agreement with those derived on the basis of our more sophisticated numerical models, which fit a much larger body of observational data for low-redshift spirals. Most importantly, they are also in fair agreement with the 'photometric' ages derived in a completely independent way and with a different sample by Bell & de Jong (2000).

In summary, our data, taken at face value, suggest that *the bulk of stars in more massive discs are older than in less massive ones*. This is supported by our detailed numerical models of galactic chemical and photometric evolution, but also by recent, independent, analysis (Boselli et al. 2001). We notice that Bell & de Jong (2000) conclude that it is local surface density that mainly drives the star formation history, while mass plays a less important role. Our study suggests that mass is the main factor, while local surface density plays only a minor role (through the spin parameter λ: lower λ values lead to higher local surface densities for a given rotational velocity V_C).

We notice that this picture is hardly compatible with the

currently popular 'paradigm' of hierarchical galaxy formation, which holds that large discs are formed by merging of small units at relatively late epochs. If this were the case, massive discs should have large SF efficiencies, in order to have their gas fractions reduced to lower levels than their less massive counterparts. However, such an enhanced SF efficiency is not supported by observations.

REFERENCES

Bell E., de Jong R., 2000, MNRAS, 312, 497
Binggeli B., Sandage A., Tammann G., 1985, AJ, 90, 1681
Boissier S., Prantzos N., 1999, MNRAS, 307, 857 (Paper I)
Boissier S., Prantzos N., 2000, MNRAS, 312, 398 (Paper II)
Boselli A., Tuffs R., Gavazzi G., Hippelein H., Pierini D., 1997a, A&AS, 121, 507
Boselli A., Gavazzi G., Lequeux J., Buat V., Casoli F., Dickey J., Donas J., 1997b, A&A, 327, 522
Boselli A., Gavazzi G., Donas J., Scodeggio M., 2001, AJ, in press
Charbonnel C., Meynet G., Maeder A., Schaerer D., 1996, A&AS, 115, 339
Cole S., Lacey C., Baugh C., Frenk C., 2000, MNRAS, 319, 168
Digel S., Grenier I., Heithausen A., Hunter S., Thaddeus P., 1996, ApJ, 463, 609
Gavazzi G., 1987, ApJ, 320, 96
Gavazzi G., Boselli A., 1996, Astrophys. Lett. Commun., 35, 1
Gavazzi G., Scodeggio M., 1996, A&A, 312, L29
Gavazzi G., Pierini D., Boselli A., 1996, A&A, 312, 397
Gavazzi G., Carrasco L., Galli R., 1999a, A&AS, 136, 227
Gavazzi G., Boselli A., Scodeggio M., Pierini D., Belsole E., 1999b, MNRAS, 304, 595
Guiderdoni B., Hivon E., Bouchet R., Maffei B., 1998, MNRAS, 295, 877
Haynes M., Giovanelli R., 1984, AJ, 89, 758
Kennicutt R., 1998a, ARA&A, 36, 189
Kennicutt R., 1998b, ApJ, 498, 541
Kroupa P., Tout C., Gilmore G., 1993, MNRAS, 262, 545
Lejeune T., Cuisinier F., Buser R., 1997, A&AS, 125, 229
McGaugh S., de Blok W., 1997, ApJ, 481, 689
Matteucci F., Greggio L., 1986, A&A, 154, 279
Mo H., Mao S., White S., 1998, MNRAS, 295, 319 (MMW98)
Navarro J. F., Steinmetz M., 1999, ApJ, 513, 555
Pagel B., 1997, Nucleosynthesis and Galactic Chemical Evolution. Cambridge Univ. Press, Cambridge
Prantzos N., 2000, in Favata F., Kaas A., Wilson A., eds, Proc. 33rd ESTEC Symp., Star Formation from the Small to the Large Scale, ESA SP-445. ESA Publications Division, Noordwijk, p. 61
Prantzos N., Boissier S., 2000, MNRAS, 313, 338 (Paper III)
Renzini A., Voli A., 1981, A&A, 94, 175
Schaller G., Schaerer D., Maeder A., Meynet G., 1992, A&AS, 96, 269
Sommer-Larsen J., Gelato S., Vedel H., 1999, ApJ, 519, 501
Woosley S., Weaver T., 1995, ApJS, 101, 181
Wyse R., Silk J., 1989, ApJ, 339, 700
Zwicky F., Herzog E., Karpowicz M., Kowal C., Wild P., 1961–68, Catalogue of Galaxies and of Clusters of Galaxies. California Institute of Technology, Pasadena (CGCG)

This paper has been typeset from a TEX/LATEX file prepared by the author.